A finite volume method for a convection- diffusion equation involving a Joule term

Caterina Calgaro, Emmanuel Creusé

A finite volume method for a convection-diffusion equation involving a Joule term

Caterina Calgaro and Emmanuel Creusé

Abstract This work is devoted to a Finite Volume method to approximate the solution of a convection-diffusion equation involving a Joule term. We propose a way to discretize this so-called "Joule effect" term in a consistent way with the non linear diffusion one, in order to ensure some maximum principle properties on the solution. We then investigate the numerical behavior of the scheme on two original benchmarks.

Key words: Finite Volume scheme - Joule term - Maximum principle.

MSC (2010)**:** 65M08 - 65M60

1 Introduction

In this work, we are interested in a convection-diffusion equation involving a Joule term, given by :

$$\partial_t u + \nabla \cdot (u\,\mathbf{v}) + 2\lambda |\nabla u|^2 - \lambda \nabla \cdot (u \nabla u) = f \quad \text{in } \Omega \times]0,T[, \tag{1}$$

$$u(\mathbf{x},0) = u_0(\mathbf{x}) \quad \text{in } \Omega, \tag{2}$$

where Ω is a polygonal open bounded subset of $\mathbb{R}^2$, $T \in \mathbb{R}_*^+$, $\lambda \in \mathbb{R}_*^+$, $\mathbf{v}$ is a divergence-free velocity field, and f the right-hand-side. The system (1)-(2) is completed with boundary conditions, given by:

Caterina Calgaro
Univ. Lille, CNRS, UMR 8524, Inria - Laboratoire Paul Painlevé, F-59000 Lille, France
e-mail: caterina.calgaro@univ-lille.fr

Emmanuel Creusé
Univ. Poly. Hauts-de-France, EA 4015, LAMAV, FR CNRS 2956, F-59313, Valenciennes, France
e-mail: emmanuel.creuse@uphf.fr

$$\begin{array}{rl} u(\mathbf{x},t) = u_D(\mathbf{x},t) & \forall\, \mathbf{x} \in \Gamma_D,\ \forall t \in]0,T[, \\ \nabla u(\mathbf{x},t)\cdot\mathbf{n} = 0 & \forall\, \mathbf{x} \in \Gamma_N,\ \forall t \in]0,T[, \end{array} \tag{3}$$

where u_D is a given function corresponding to non homogeneous Dirichlet boundary conditions, $\overline{\Gamma_D} \cup \overline{\Gamma_N} = \overline{\Gamma} = \overline{\partial\Omega}$ and $\Gamma_D \cap \Gamma_N = \emptyset$.

System (1)-(2)-(3) (with $f = 0$) can be derived in the context of low-Mach modeling. Taking into account the compressible Navier-Stokes system where an asymptotic development of the pressure with respect to the Mach number is done, we start by considering the mass conservation equation

$$\partial_t \rho + \nabla\cdot(\rho\,\mathbf{V}) = 0,$$

where $\rho(\mathbf{x},t)$ is the density and $\mathbf{V}(\mathbf{x},t)$ the velocity field of the fluid. In the case of the ideal gas law $P_0 = R\rho u$, where $u(\mathbf{x},t)$, $P_0 > 0$ and $R > 0$ stand respectively for the temperature, the constant thermodynamic pressure and the ideal gas constant, a solenoidal velocity field $\mathbf{v}(\mathbf{x},t)$ can be introduced. It is shown in [3] that the change of variable $\mathbf{v} = \mathbf{V} - \lambda\nabla u$ leads to equation (1), where $\lambda > 0$ is a fixed constant which depends on the constant heat conductivity $k > 0$ in the nonstandard constraint

$$P_0 \nabla\cdot\mathbf{V} = R\,\nabla\cdot(k\nabla u)$$

introduced in the low-Mach model. In [3] a particular dynamic viscosity is also introduced, defined by $\mu(u) = -\lambda \ln u$, in order to remove the $O(\lambda^2)$ terms in the momentum equation. With this choice, $\mu(u)$ is strictly positive if and only if $u \in (0,1)$. However, in this work we assume only that there exist two real numbers m and M such that $0 < m \leq u_0(\mathbf{x}) \leq M < +\infty$ a.e. $\mathbf{x} \in \Omega$.

From the theoretical point of view, several results have been obtained for the system (1)-(2)-(3). For instance, the local-in-time existence of strong solutions has been established in [3] in the framework of a coupling with the Navier-Stokes system. In particular, a maximum-principle has been derived (see [6], Theorem 5.1). This formulation is also related to others obtained in the context of the so-called ghost effect system, where a thermal stress term is added to the right-hand-side of the momentum equation, for which some results on the existence and uniqueness of solutions are available [10, 9].

From the numerical point of view, in the context of Finite Volume schemes, an important question to be addressed consists in the way to discretize the Joule term $|\nabla u|^2$ arising in (1) in each control volume, in a consistent way with the non linear diffusion one. It has to be done in order to ensure some properties on the numerical solution, such as some maximum principles which hold at the continuous level. Several possibilities have already been investigated in the context of the electrical conductivity (see for example [1, 5, 4]) but, to our knowledge, never for the model (1)-(2)-(3).

In this work, we present a finite volume scheme for the discretization of (1)-(2)-(3) which has been initially introduced in [2]. The aim of the present contribution is to give some results in the case $f \neq 0$, and to investigate the efficiency of the derived scheme (as well as a variant one) on two original benchmarks. More precisely, we first illustrate our theoretical results on a discontinuous solution submitted to a solenoidal convective velocity field. Then, we consider a regular analytical solution for which the right-hand-side is positive, in order to investigate the lower bound preserving property of the numerical solution as well as the convergence process.

2 Finite Volume Scheme

2.1 Notations

As usual, the discretization in space is based on a triangulation $\mathcal{T}$ of the domain $\Omega \subset \mathbb{R}^2$, a family $\mathcal{E}$ of edges and a set $\mathcal{P} = (\mathbf{x}_K)_{K\in\mathcal{T}}$ of points of Ω defining an admissible mesh in the sense of Definition 3.1 in [7]. We recall that the admissibility of $\mathcal{T}$ implies that the straight line between two neighboring centers of cells $\mathbf{x}_K$ and $\mathbf{x}_L$ is orthogonal to the edge $\sigma \in \mathcal{E}$ such that $\overline{\sigma} = \overline{K} \cap \overline{L}$ (and which is noted $\sigma = K|L$) in a point $\mathbf{x}_\sigma$.

The set of interior (resp. boundary) edges is denoted by $\mathcal{E}^{\text{int}} = \{\sigma \in \mathcal{E} \ ; \ \sigma \notin \Gamma\}$ (resp. $\mathcal{E}^{\text{ext}} = \{\sigma \in \mathcal{E} \ ; \ \sigma \subset \Gamma\}$). Among the outer edges, there are $\mathcal{E}^N = \{\sigma \in \mathcal{E} \ ; \ \sigma \subset \Gamma_N\}$ and $\mathcal{E}^D = \{\sigma \in \mathcal{E} \ ; \ \sigma \subset \Gamma_D\}$. For all $K \in \mathcal{T}$, we denote by $\mathcal{E}_K = \left\{\sigma \in \mathcal{E} \ ; \ \sigma \subset \overline{K}\right\}$ the edges of K, $\mathcal{E}_K^{\text{int}} = \mathcal{E}^{\text{int}} \cap \mathcal{E}_K$, $\mathcal{E}_K^{\text{ext}} = \mathcal{E}^{\text{ext}} \cap \mathcal{E}_K$, $\mathcal{E}_K^N = \mathcal{E}_K^N \cap \mathcal{E}_K$ and $\mathcal{E}_K^D = \mathcal{E}_K^D \cap \mathcal{E}_K$.

The measure of $K \in \mathcal{T}$ is denoted by m_K and the length of σ by m_σ. For $\sigma \in \mathcal{E}^{\text{int}}$ such that $\sigma = K|L$, d_σ denotes the distance between $\mathbf{x}_K$ and $\mathbf{x}_L$ and $d_{K,\sigma}$ the distance between $\mathbf{x}_K$ and σ. For $\sigma \in \mathcal{E}_K^{\text{ext}}$, we note d_σ the distance between $\mathbf{x}_K$ and σ. For $\sigma \in \mathcal{E}$, the transmissibility coefficient is given by $\tau_\sigma = \dfrac{m_\sigma}{d_\sigma}$. Finally, for $\sigma \in \mathcal{E}_K$, we denote by $\mathbf{n}_{K,\sigma}$ the exterior unit normal vector to σ. The size of the mesh is given by:

$$h = \max_{K\in\mathcal{T}} \text{diam}(K).$$

We define a partition of the time interval $(0, T)$ such that $0 = t^0 < \cdots < t^n < \cdots < t^N = T$ ($N \in \mathbb{N}^*$), and we denote $\Delta t_n = t^{n+1} - t^n$ for $0 \leq n \leq N-1$. Here, u_K^n denotes the value of the numerical solution $u_h^n = (u_K^n)_{K\in\mathcal{T}}$ in K and in the time interval $[t^n, t^{n+1}[$.

2.2 The Finite Volume scheme 1

The Finite Volume scheme for the discretization of (1)-(2)-(3) is given by integrating (1) on a control volume K to obtain:

$$m_K \frac{u_K^{n+1} - u_K^n}{\Delta t_n} + \sum_{\sigma \in \mathcal{E}_K} v_{K,\sigma}^n \, u_{K\,\sigma,+}^{n+1} + 2\lambda m_K \mathcal{J}_K(u_h^{n+1}) + \lambda \sum_{\sigma \in \mathcal{E}_K} F_{K,\sigma}^{n+1} = m_K f_K^{n+1} \quad \forall K \in \mathcal{T}, \tag{4}$$

with

$$v_{K,\sigma}^n = \int_\sigma \mathbf{v}(\mathbf{x}, t^n) \cdot \mathbf{n}_{K,\sigma} \, \mathrm{d}\gamma(\mathbf{x}) \quad \text{and} \quad f_K^{n+1} = \frac{1}{m_K} \int_K f(\mathbf{x}, t^{n+1}) \, \mathrm{d}\mathbf{x}.$$

Here, $u_{K\,\sigma,+}^{n+1}$ is defined for $\sigma \in \mathcal{E}_K$ by:

$$u_{K\,\sigma,+}^{n+1} = \begin{cases} u_K^{n+1} & \text{if } v_{K,\sigma}^n \geq 0, \\ u_{K,\sigma}^{n+1} & \text{otherwise,} \end{cases}$$

with

$$u_{K,\sigma}^{n+1} = \begin{cases} u_L^{n+1} & \text{for } \sigma \in \mathcal{E}_K^{\text{int}} \text{ such that } \sigma = K|L, \\ u_D^{n+1}(\mathbf{x}_\sigma) & \text{for } \sigma \in \mathcal{E}_K^D, \\ u_K^{n+1} & \text{for } \sigma \in \mathcal{E}_K^N. \end{cases}$$

The numerical flux $F_{K,\sigma}^{n+1}$ is an approximation of the exact flux of the non linear diffusion term through the edge σ, given classically by:

$$F_{K,\sigma}^{n+1} = \frac{\tau_\sigma}{2} \left((u_K^{n+1})^2 - (u_{K,\sigma}^{n+1})^2 \right). \tag{5}$$

Concerning the Joule term, $\mathcal{J}_K(u_h^{n+1})$ is an approximation of $\frac{1}{m_K} \int_K |\nabla u(\mathbf{x}, t^{n+1})|^2 \mathrm{d}\mathbf{x}$. A first idea may be to consider a scheme also centered for this term, in order to increase the accuracy of the approximation, by following the piecewise discrete gradient introduced in [8], for instance. Nevertheless, we have shown in [2] that with this choice, a discrete maximum principle is only verified under very restrictive conditions on the initial data. A more effective approach is to consider an upwind discretization of the Joule term defined by:

$$\mathcal{J}_K(u_h^{n+1}) = \frac{1}{m_K} \sum_{\sigma \in \mathcal{E}_K} \tau_\sigma \left((u_K^{n+1} - u_{K,\sigma}^{n+1})^+ \right)^2, \tag{6}$$

where we use the notation $a^+ = \max(0, a)$. We give now the main result :

Theorem 1. *We assume that*

$$0 < m \leq u_K^0 \leq M \quad \forall K \in \mathcal{T} \;\; \textit{and} \;\; 0 < m \leq u_D^n(\boldsymbol{x}_\sigma) \leq M, \quad \forall \sigma \in \mathcal{E}^D, \forall n = 1, \cdots, N.$$

We suppose moreover that:

$$f_K^n \geq 0 \quad \forall K \in \mathcal{T}, \forall n = 1, \cdots, N.$$

Then the scheme (4) admits at least one solution that satisfies :

$$m \leq u_K^n \leq M + T\,\|f\|_{L^\infty(\Omega\times[0,T])}, \quad \forall K \in \mathcal{T}, \forall n = 1, \cdots, N. \tag{7}$$

Proof. The proof consists in an extension of the proof of Theorem 3.1 in [2] established in the case $f \equiv 0$, noticing in particular that $((u_K^{n+1} - u_{K,\sigma}^{n+1})^+)^2 = 0$ if $u_K^{n+1} \leq u_{K,\sigma}^{n+1}$. First, we prove that for any solution of (4), estimation (7) holds. Then, we use a topological degree argument to establish the existence of the solution.

Remark 1. In the case $f_K^n \leq 0$, a similar result can also be obtained. Concerning the upper bound, it can easily be proved that any solution of (4) satisfies $u_K^n \leq M$, $\forall K \in \mathcal{T}, \forall n = 1, \cdots, N$. Concerning the lower bound, the time T has to be chosen sufficiently small to ensure that $u_K^n > 0$, $\forall K \in \mathcal{T}, \forall n = 1, \cdots, N$ and to be able to prove the existence of the solution.

2.3 A variant: Scheme 2

Here, we propose a variant of the previous numerical scheme. First, we would like to suggest a centered treatment of the Joule term instead of (6). It is worth noticing that $|\nabla u|^2 = \nabla \cdot (u \nabla u) - u \Delta u$, then we propose the following definition:

$$\mathcal{J}_K(u_h^{n+1}) = \frac{1}{m_K} \sum_{\sigma \in \mathcal{E}_K} \tau_\sigma \overline{u}_\sigma^{n+1} \left(u_{K,\sigma}^{n+1} - u_K^{n+1}\right) - \frac{1}{m_K} u_K^{n+1} \sum_{\sigma \in \mathcal{E}_K} \tau_\sigma \left(u_{K,\sigma}^{n+1} - u_K^{n+1}\right),$$

where $\overline{u}_\sigma^{n+1}$ is an approximation of u^{n+1} at $\mathbf{x}_\sigma$ defined by: $\overline{u}_\sigma^{n+1} = \dfrac{u_K^{n+1} + u_{K,\sigma}^{n+1}}{2}$. Finally we obtain:

$$\mathcal{J}_K(u_h^{n+1}) = \frac{1}{2m_K} \sum_{\sigma \in \mathcal{E}_K} \tau_\sigma (u_{K,\sigma}^{n+1} - u_K^{n+1})^2.$$

With this choice, if we hope to achieve a maximum principle without restrictions on the data, we need to reach a balance between the Joule term and the diffusive one. Thus, instead of (5), we propose to define the numerical flux for the diffusion term through the edge σ by:

$$F_{K,\sigma}^{n+1} = \tau_\sigma\, u_\sigma^{n+1} (u_K^{n+1} - u_{K,\sigma}^{n+1}),$$

where u_σ^{n+1} is another approximation of u^{n+1} at $\mathbf{x}_\sigma$ defined this time by: $u_\sigma^{n+1} = \max(u_K^{n+1}, u_{K,\sigma}^{n+1})$. Provided this balance between the diffusion term and the Joule one, Theorem 1 occurs.

3 Benchmarks

3.1 Maximum Principle : case $f = 0$

This first benchmark consists in solving (1)-(2)-(3) with $\Omega = [0;1]^2$ for $0 \leq t \leq T = 0.1$, with $f \equiv 0$, $\lambda = 2$, $\Gamma_D = \Gamma$, $\Gamma_N = \emptyset$ and $\forall t \in [0;T]$:

$$u_D(\mathbf{x},t) = \begin{cases} 1 & \text{if } \mathbf{x} \in \Gamma \backslash \Gamma_H, \\ M & \text{if } \mathbf{x} \in \Gamma_H, \end{cases} \quad M > 1,$$

where $\Gamma_H = \{1\} \times (0,3;0,7)$. Moreover, the given velocity field $\mathbf{v}(\mathbf{x},t)$ is given by :

$$\mathbf{v}(\mathbf{x},t) = 5\sqrt{t}\, e^{-25\|\mathbf{x}-\mathbf{c}\|^2} \begin{pmatrix} -y+c_2 \\ x-c_1 \end{pmatrix}, \quad \forall \mathbf{x} = (x,y)^T \in \Omega, \quad \forall t \in [0,T],$$

with $\mathbf{c} = (c_1,c_2)^T = (0.5,0.5)^T$. Since $f \equiv 0$, Theorem 1 can be applied, so that the numerical solution should be bounded between 1 and M, what we aim to illustrate here. The simulations are performed on a triangulation $\mathcal{T}$ corresponding to $h = 3.62 \cdot 10^{-2}$. Since both schemes are implicit in time, a Newton solver is implemented associated with the adaptive time step Δt_n to compute u_h^{n+1} from u_h^n from (4). Iterations are performed until the accuracy on the residual in l^∞-norm is less than 10^{-10}. If it is not the case after 15 iterations, the time step is divided by 2 and the resolution is done again. Conversely, the solver tries to multiply by a factor 2 the time step periodically. Several values of M are considered from $M = 2$ to $M = 50$. Results are displayed in Table 1. On the one hand, it is observed that the numerical solution is bounded between 1 and M whatever the value of M chosen, as theoretically expected. On the other hand, we investigate the time steps Δt_{min} and Δt_{max}, corresponding respectively to the smallest and the largest value of Δt_n used in $[0,T]$. First, it can be seen that the higher M is, the smaller Δt_{min} and Δt_{max} have to be in order to ensure the convergence process. Then, we remark that Scheme 1 leads to a value of Δt_{max} roughly ten times larger than the one used for Scheme 2, and consequently to a faster computation of the solution on the interval $[0,T]$.

Table 1 Verification of the maximum principle according to M. ✓ : it is satisfied.

$M =$		Scheme 1			Scheme 2	
		Δt_{min}	Δt_{max}		Δt_{min}	Δt_{max}
2	✓	$6.25 \cdot 10^{-5}$	$5.00 \cdot 10^{-4}$	✓	$7.81 \cdot 10^{-6}$	$1.56 \cdot 10^{-5}$
10	✓	$3.91 \cdot 10^{-6}$	$3.13 \cdot 10^{-5}$	✓	$1.95 \cdot 10^{-6}$	$3.91 \cdot 10^{-6}$
20	✓	$1.95 \cdot 10^{-6}$	$1.56 \cdot 10^{-5}$	✓	$6.25 \cdot 10^{-7}$	$2.50 \cdot 10^{-6}$
50	✓	$4.88 \cdot 10^{-7}$	$7.81 \cdot 10^{-6}$	✓	$2.50 \cdot 10^{-7}$	$5.00 \cdot 10^{-7}$

3.2 Convergence rate and Maximum Principle : case $f \neq 0$

Now, we want to investigate numerically the convergence rate of the schemes on a regular solution and to illustrate Theorem 1 in one case corresponding to $f \neq 0$. To do that, we consider the exact solution u_{ex} given by:

$$u_{ex}(\mathbf{x},t) = \sin\Big(t+\frac{\pi}{6}\Big)(5-x^2(x+y)^2)$$

for $\mathbf{x} = (x,y)^T \in \Omega = [0;1]^2$ and $0 \leq t \leq T = 0.1$, where the given velocity field is:

$$\mathbf{v}(\mathbf{x},t) = \cos(t)\begin{pmatrix} -x^2(x-1)^2(y-1)(y-0.5)y \\ y^2(y-1)^2(x-1)(x-0.5)x \end{pmatrix}, \quad \forall \mathbf{x} = (x,y)^T \in \Omega, \quad \forall t \in [0,T].$$

In the computation, we define $\Gamma_N = \{0\}\times[0,1]$ and $\Gamma_D = \Gamma \backslash \Gamma_N$. We set $\lambda = 1$ and the value of f in (1) is being computed accordingly. It can easily be checked that $f \geq 0$ in $\Omega \times [0,T]$, so that Theorem 1 ensures that the numerical solution u_h has to remain bounded from below during the whole simulation by:

$$m = \min_{\mathbf{x}\in\Omega} u_{ex}(\mathbf{x},0) = 0.5. \tag{8}$$

Simulations are performed on triangulations $\mathcal{T}_i$ ($i = 1,\dots 6$), so that $h = 0.145$ for $\mathcal{T}_1$, and the value of h is twice smaller for $\mathcal{T}_i$ than for $\mathcal{T}_{i-1}$ ($2 \leq i \leq 6$). First, we observe that whatever the simulation considered, u_h remains bounded from below by m defined by (8), as theoretically expected. Then, the error in $L^\infty(0,T;\Omega)$ norm is plotted in Figure 1 as a function of the mesh size h, in log-log scale. We observe that both schemes are first-order accurate in space. This behavior was clearly expected because of the upwind treatment of the convective term, but also because of the upwind choice in the Joule term (in Scheme 1) or in the diffusion term (in Scheme 2), required to obtain the estimation (7). We observe that the convergence rate is the same and that Scheme 1 leads to a value of Δt_n two orders of magnitude larger than the one used for Scheme 2 in order to make the Newton algorithm converging, even if Scheme 2 seems a little bit more accurate than Scheme 1. The advantage of Scheme 1 is confirmed also considering smaller values of λ, or smaller magnitude of $\mathbf{v}$ or u_{ex}. Finally, other schemes have been proposed and analyzed in [2]. Even if they are of order two in the case $\mathbf{v} = 0$, they verify the maximum principle only under very restrictive conditions on the magnitude of $M - m$.

Acknowledgements This work was supported in part by the Labex CEMPI (ANR-11-LABX-0007-01).

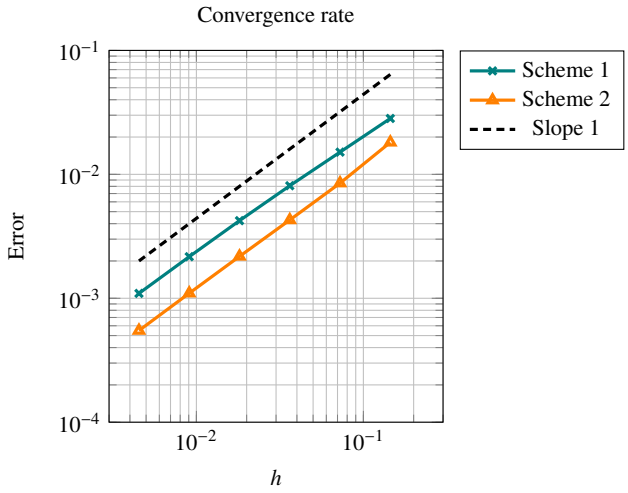

Fig. 1 Errors in $L^\infty(0,T;\Omega)$ norm.

References

1. Bradji, A., Herbin, R.: Discretization of coupled heat and electrical diffusion problems by finite-element and finite-volume methods. IMA J. Numer. Anal. **28**(3), 469–495 (2008). DOI 10.1093/imanum/drm030. URL https://doi.org/10.1093/imanum/drm030
2. Calgaro, C., Colin, C., Creusé, E.: A combined finite volume - finite element scheme for a low-Mach system involving a Joule term. AIMS Mathematics **5**(1), 311–331 (2020). DOI 10.3934/math.2020021
3. Calgaro, C., Colin, C., Creusé, E., Zahrouni, E.: Approximation by an iterative method of a low-Mach model with temperature dependant viscosity. Math. Methods Appl. Sci. **42**, 250–271 (2019)
4. Chainais-Hillairet, C.: Discrete duality finite volume schemes for two-dimensional drift-diffusion and energy-transport models. Internat. J. Numer. Methods Fluids **59**(3), 239–257 (2009). DOI 10.1002/fld.1393. URL https://doi.org/10.1002/fld.1393
5. Chainais-Hillairet, C., Peng, Y.J., Violet, I.: Numerical solutions of Euler-Poisson systems for potential flows. Appl. Numer. Math. **59**(2), 301–315 (2009). DOI 10.1016/j.apnum.2008.02.006. URL https://doi.org/10.1016/j.apnum.2008.02.006
6. Colin, C.: Analyse et simulation numérique par méthode combinée volumes finis - eléments finis de modèles de type faible mach. Ph.D. thesis, Université de Lille (2019)
7. Eymard, R., Gallouët, T., Herbin, R.: Finite volume methods. In: Handbook of numerical analysis, Vol. VII, Handb. Numer. Anal., VII, pp. 713–1020. North-Holland, Amsterdam (2000)
8. Eymard, R., Gallouët, T., Herbin, R.: A cell-centered finite-volume approximation for anisotropic diffusion operators on unstructured meshes in any space dimension. IMA J. Numer. Anal. **26**(2), 326–353 (2006). DOI 10.1093/imanum/dri036. URL https://doi.org/10.1093/imanum/dri036
9. Huang, F., Tan, W.: On the strong solution of the ghost effect system. SIAM J. Math. Anal. **49**(5), 3496–3526 (2017). DOI 10.1137/16M106964X. URL https://doi.org/10.1137/16M106964X
10. Levermore, C., Sun, W., Trivisa, K.: Local well-posedness of a ghost system effect. Indiana Univ. Math. J. **60**, 517–576 (2011)